



# MEaSURES BedMachine Antarctica, Version 4

---

## USER GUIDE

### How to Cite These Data

As a condition of using these data, you must include a citation:

Morlighem, M. (2025). *MEaSURES BedMachine Antarctica* (NSIDC-0756, Version 4). [Data set]. Boulder, Colorado USA. NASA National Snow and Ice Data Center Distributed Active Archive Center. <https://doi.org/10.5067/POJQI54A45HX>. [Date Accessed].

We also request that you acknowledge the author(s) of this data set by referencing the following peer-reviewed publication:

Morlighem, M., Rignot, E., Binder, T., Blankenship, D. D., Drews, R., Eagles, G., et al. (2020). Deep glacial troughs and stabilizing ridges unveiled beneath the margins of the Antarctic ice sheet. *Nature Geoscience*, 13, 132–137. <https://doi.org/10.1038/s41561-019-0510-8>

FOR QUESTIONS ABOUT THESE DATA, CONTACT [NSIDC@NSIDC.ORG](mailto:NSIDC@NSIDC.ORG)

FOR CURRENT INFORMATION, VISIT <https://nsidc.org/data/NSIDC-0756>



National Snow and Ice Data Center

# TABLE OF CONTENTS

1	DATA DESCRIPTION.....	2
1.1	Parameters .....	2
1.2	File Information .....	2
1.2.1	Format .....	2
1.2.2	File Contents .....	2
1.2.3	Naming Convention .....	4
1.3	Spatial Information .....	4
1.3.1	Coverage .....	4
1.3.2	Resolution.....	4
1.3.3	Geolocation .....	4
1.4	Temporal Information .....	4
1.4.1	Coverage .....	4
2	DATA ACQUISITION AND PROCESSING .....	4
2.1	Acquisition.....	4
2.2	Ice Thickness Mapping .....	6
2.2.1	Firn Air Correction .....	7
2.3	Data Quality and Errors.....	8
3	VERSION HISTORY .....	8
4	REFERENCES .....	9
5	DOCUMENT INFORMATION.....	11
5.1	Publication Date .....	11
5.2	Date Last Updated .....	11

# 1 DATA DESCRIPTION

## 1.1 Summary

---

This data set contains a bed topography and bathymetry map of Antarctica. Bed topography is deduced by subtracting ice thickness from the surface elevation; using Ice Flow Perturbation Analysis (IFPA); and by other methods. Surface elevations are obtained from the Reference Elevation Model of Antarctica (REMA) and high-resolution satellite maps.

## 1.2 File Information

---

### 1.2.1 Format

NetCDF-4

### 1.2.2 File Contents

This data set consists of a single NetCDF file. Ice thickness and ice surface elevations are reported in ice equivalent (heights above mean sea level using the EIGEN-6C4 geoid<sup>1</sup>) to account for firn air content. Errors in the ice thicknesses/bed topography are also provided. Additional parameters include firn air content; EIGEN-6C4 geoid height difference from the WGS84 ellipsoid; and an ice/ocean/land mask. A source map is also provided that shows where each method was applied.

All parameters included in the data file are described in Table 1 below:

Table 1. File Parameter Descriptions

Parameter	Description
bed	Bed elevation (bed topography) relative to the EIGEN-6C4 geoid (m)
dataid	Input data source ID: 0 = no data; 1 = radar seismic multibeam (REMA); 2 = radar; 7 = seismic; 10 = multibeam
errbed	Ice thickness/bed topography error (m)
firn	Firn air content (m)
geoid	Geoid height difference (m) from WGS84 ellipsoid (EIGEN-6C4 – WGS 84) <sup>2</sup>

---

<sup>1</sup> See Förste et al., 2014.

<sup>2</sup> To obtain height above the WGS84 ellipsoid, add the value in the “geoid” parameter to the value in the “bed” parameter at the same location.

Parameter	Description
mapping	Grid mapping variable with a complete description of the coordinate reference system.
mask	Ice/ocean/land mask: 0 = ocean; 1 = ice-free land; 2 = grounded ice; 3 = floating ice; 4 = Lake Vostok
rgi	Randolph Glacier Inventory (RGI) mask (v7.0)
source	Output data source ID. 1 = REMA/IBCSO v2; 2 = mass conservation; 3 = interpolation; 4 = hydrostatic; 5 = IFPA; 6 = gravity; 7 = seismic; 8 = IceBoost; 10 = multibeam
surface	Ice surface elevation (m)
thickness	Ice thickness (m)
x	Projection x coordinate (m)
y	Projection y coordinate (m)

The following figure shows an example of how the bed topography and ice thickness can be mapped:

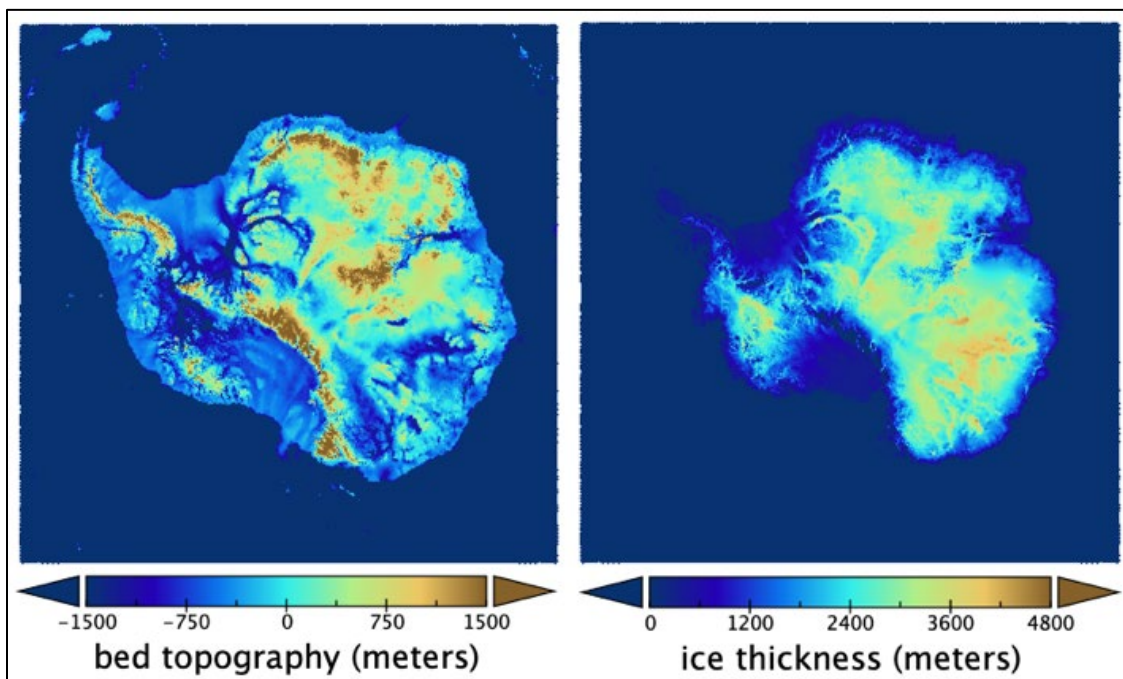


Figure 1. Maps of bed topography (left) and ice thickness (right).

### 1.2.3 Naming Convention

The data set consists of a single file named:

NSIDC-0756\_BedMachineAntarctica\_19700101-20191001\_V04.1.nc

ⓘ The first public release of this Version 4 data set is V4.1 (indicated by “V04.1” in the file name), following the convention established by the data provider.

## 1.3 Spatial Information

---

### 1.3.1 Coverage

N: 53° S

S: 90° S

E: 180° E

W: 180° W

### 1.3.2 Resolution

500 m

### 1.3.3 Geolocation

Data are provided in the WGS 84 / Antarctic Polar Stereographic projection ([EPSG:3031](#)). For details about the EIGEN-6C4 geoid, see Förste et al, 2014.

## 1.4 Temporal Information

---

### 1.4.1 Coverage

The data were collected between 1 January 1970 and 1 October 2019. The nominal year of this data set, 2015, refers to the year of the reference surface digital elevation model.

## 2 DATA ACQUISITION AND PROCESSING

### 2.1 Acquisition

---

This data set was generated from the following input data:

- Ice thickness from 1967 to 2020 obtained by 47 airborne ice penetrating radar survey campaigns (see Figure 2). Additional sources of ice thickness data include:
  - The Center for Remote Sensing and Integrated Systems (CReSIS) 2018 and 2019 data
  - British Antarctic Survey Polarimetric radar Airborne Science Instrument (PASIN) data
  - Young et al. (2017) and Cui et al. (2020) for constraining bed topography under grounded ice
  - Smith et al. (2020) for thinning rates
  - IceBoost for periphery glaciers and peninsula (Maffezzoli et al., 2025)
- Ice flow velocity derived from satellite interferometry (Rignot et al., 2011; Mouginot et al., 2017)
- Surface mass balance obtained with a regional atmospheric climate model (RACMO2; van Wessem et al., 2018), representative of the period 1961–1990
- Surface topography from REMA (Howat et al., 2019)
- The International Bathymetric Chart of the Southern Ocean (IBCSO) v2
- Multi-beam ocean bathymetry data in the Amundsen Sea embayment (Hogan et al., 2020) as well as gravity inversions for this sector (Jordan et al., 2020).
- Ocean bathymetry from Gravity and Geoid in Antarctica (AntGG) along parts of the coast (Charrassin et al., 2025) and IBCSO v2 (Dorschel et al., 2022)
- Ice Flow Perturbation Analysis to map the bed in the interior (Ockenden et al., 2023)

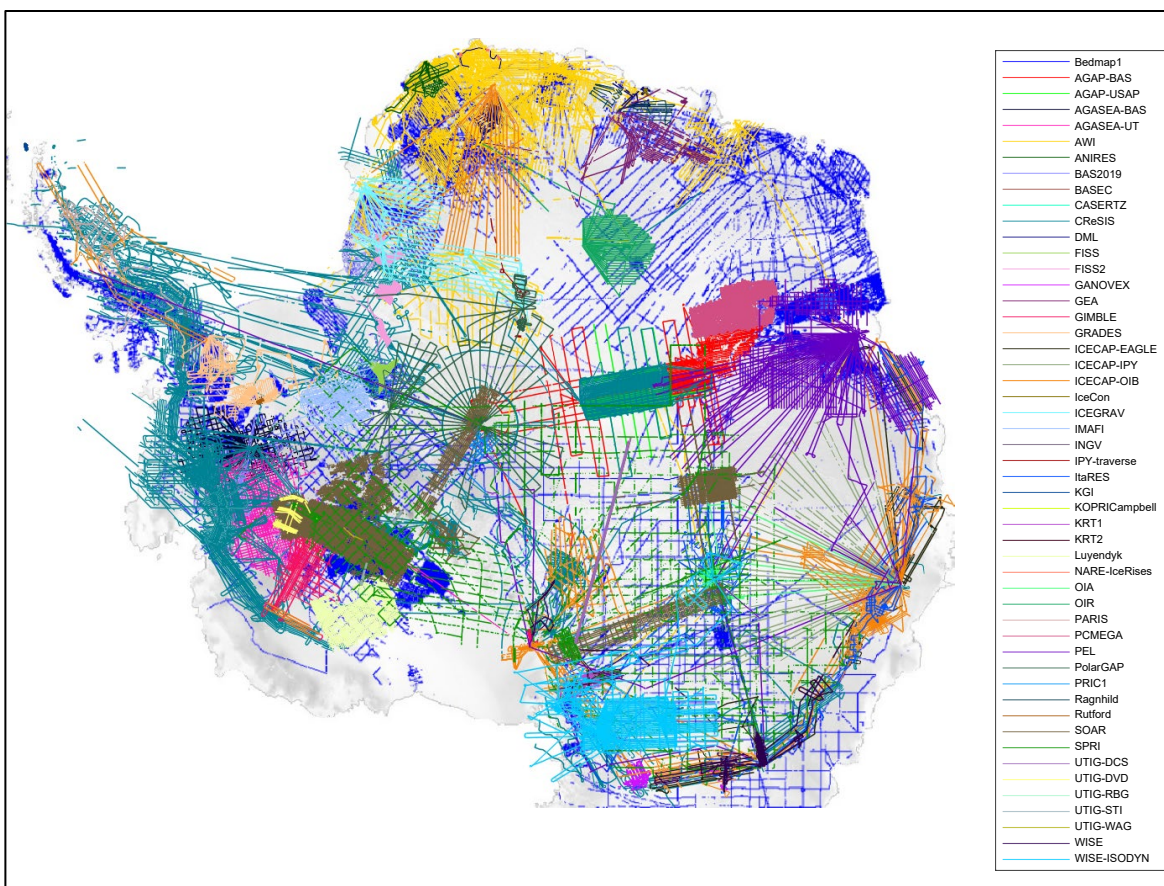


Figure 2. Ice thicknesses were mainly derived from 47 airborne ice penetrating radar survey campaigns flown between 1967 and 2020. References and the institutions involved in each campaign (plotted above) are available in “Table S1,” Morlighem et al. (2020).

## 2.2 Processing

### 2.2.1 Ice Thickness Mapping

Different methods were used to map ice thickness, depending on the ice characteristics: mass conservation in regions of fast-moving ice; IFPA in regions of slow-moving ice; hydrostatic equilibrium for floating ice shelves; and gravity inversion and seismic bathymetry for grounded ice shelves.

#### 2.2.1.1 Mass Conservation (MC)

Ice surface motion offers a physical basis to extrapolate sparse ice thickness data to areas with little or no data. The method works best in well-confined regions of fast flow (ice surface velocity > 30 m/yr), where errors in flow direction are small and glaciers slide on the bed. The MC method yields ice thickness and bed topography that compares favorably with ice sheet numerical models; resolves uncertainties in previous estimates interpreted from radar echoes; and ensures that

grounding-line fluxes are compatible with snowfall accumulation and thinning rates in the interior, without assuming steady-state conditions.

The MC method combines sparse, airborne, radar-sounding-derived ice thickness data with high-resolution ice motion derived from satellite interferometric synthetic-aperture radar and mass balance to estimate ice thickness across the entire continent. The algorithm conserves mass fluxes while minimizing the departure from the original radar-derived ice thickness data. The method is summarized in Morlighem et al. (2019, Supplementary Information) and extensively detailed in Morlighem et al. (2011, 2014, 2017).

### 2.2.1.2 Ice Flow Perturbation Analysis (IFPA)

IFPA was applied in the interior, slow-moving sectors, where errors in flow direction are larger. IFPA is an inverse method that leverages the physics of ice flow to invert for subglacial topography from contemporary ice surface datasets. This approach was chosen as an alternative to more commonly used methods (e.g., kriging, splines, and streamline diffusion), which struggle to reproduce the roughness of subglacial terrain observed along radar profiles or mesoscale landscapes. For a detailed description of IFPA, see Ockenden et al. (2023, 2026).

### 2.2.1.3 Hydrostatic Equilibrium

Hydrostatic equilibrium is applied to floating ice shelves, using a calibrated firn depth correction to maintain consistency between inferred ice thicknesses and available ice shelf thickness data, and to ensure continuity across the grounding line.

Once the thickness estimates are computed using the methods described above, the final product is constructed by stitching together the individual MC thickness maps, constrained by flight lines along their boundaries, using simple interpolation (inverse distance weighting). The MC maps are then combined with the thickness maps derived via streamline diffusion. Antarctic bed topography is derived by subtracting the resulting ice thickness map from the REMA surface digital elevation model (Howat et al., 2019). Over ice-free land areas, the bed topography is the REMA itself.

## 2.2.2 Firn Air Correction

Surface elevations and ice thicknesses in this data set are provided in ice equivalent, which includes a firn air content correction (i.e., elevations are lower than they would be with air column height included). The elevation of the top of the snow as provided by REMA can be reconstructed by adding the firn depth correction (firn air content) to the ice surface elevation.

## 2.3 Quality, Errors, and Limitations

Error estimates of the bed elevation and ice thickness are provided in the “errbed” variable. Sources of error include error in ice velocity direction and magnitude; error in surface mass balance; and ice thinning rates.

In a trial setting with unusually dense radar sounding coverage, errors in the MC-inferred thickness are reported at 36 m, only slightly higher than that of the original data. In areas less well constrained by radar-derived thickness data or constrained by only one track of data (e.g., in East Antarctica), errors may exceed 200 m (Morlighem et al., 2020). In areas where sparse ice shelf bathymetry are available, uncertainty may exceed 500 m.

## 3 VERSION HISTORY

Table 2. Version History Summary

Version	Date	Description of Changes
3.0 (retire)	24 Feb 2026	Version 3 retired, data access removed
4.1 <sup>3</sup>	21 Jan 2026	<ul style="list-style-type: none"> <li>• Uses Ice Flow Perturbation Analysis to map the bed in the interior (Ockenden et al., 2023)</li> <li>• Uses ice thickness estimates from IceBoost for periphery glaciers and Peninsula (Maffezzoli et al., 2025)</li> <li>• Uses ocean bathymetry from AntGG along parts of the coast (Charrassin et al., 2025) and IBCSO v2 (Dorschel et al., 2022)</li> <li>• Added a new field 'RGI' that indicates which pixel belongs to a glacier in the Randolph Glacier Inventory</li> </ul>
2.0 (retire)	22 Nov 2022	Removed data access for v2.0. Temporal coverage was 1 Jan 1970 to 1 Oct 2019.
1.0 (retire)	2 Nov 2022	Removed data access for v1.0. Temporal coverage was 1 Jan 1970 to 1 Oct 2019.
3.0	19 Oct 2022	<ul style="list-style-type: none"> <li>• Added ice thickness measurements from CReSIS 2018, CReSIS 2019, and PASIN</li> <li>• Updated thinning rates per Smith et al. (2020)</li> <li>• Added parameter (“dataid”) to more easily identify data source</li> <li>• Uses IBCSO v2 for ocean bathymetry</li> </ul>

<sup>3</sup> The first public release of this Version 4 data set is V4.1, following a convention established by the data provider.

2.0	29 Sep 2020	<ul style="list-style-type: none"> <li>• Additional thickness data to constrain the bed topography under grounded ice</li> <li>• New multi-beam bathymetry data, as well as gravity inversions, integrated in the Amundsen Sea embayment</li> <li>• An error in geoid height was corrected for the IBCSO bathymetry</li> </ul>
1.0	12 Dec 2019	Initial release

## 4 REFERENCES

Arndt, J. E., Schenke, H. W., Jakobsson, M., Nitsche, F. O., Buys, G., Goleby, B., et al. (2013). The International Bathymetric Chart of the Southern Ocean (IBCSO) Version 1.0-A new bathymetric compilation covering circum-Antarctic waters. *Geophysical Research Letters*, *40*(12), 3111–3117.

<https://doi.org/10.1002/grl.50413>

Charrassin, R., Millan, R., Rignot, E. & Scheinert, M. (2025). Bathymetry of the Antarctic continental shelf and ice shelf cavities from circumpolar gravity anomalies and other data. *Scientific Reports*, *15*. <https://doi.org/10.1038/s41598-024-81599-1>

Cui, X., Jeofry, H., Greenbaum, J. S., Guo, J., Li, L., Lindzey, L. E., Habbal, F. A., Wei, W., Young, D. A., Ross, N., Morlighem, M., Jong, L. M., Roberts, J. L., Blankenship, D. D., Bo, S., & Siegert, M. J. (2020). Bed topography of Princess Elizabeth Land in East Antarctica. *Copernicus GmbH*.

<https://doi.org/10.5194/essd-2020-126>

Dorschel, B., et al. (2022). The International Bathymetric Chart of the Southern Ocean Version 2. *Scientific Data*, *9*. <https://doi.org/10.1038/s41597-022-01366-7>

Förste, C., Bruinsma, Sean. L., Abrikosov, O., Lemoine, J.-M., Marty, J. C., Flechtner, F., Balmino, G., Barthelmes, F., & Biancale, R. (2014). EIGEN-6C4 The latest combined global gravity field model including GOCE data up to degree and order 2190 of GFZ Potsdam and GRGS Toulouse [Dataset]. GFZ Data Services. <https://doi.org/10.5880/ICGEM.2015.1>

Greenbaum, J. S., Blankenship, D. D., Young, D. A., Richter, T. G., Roberts, J. L., Aitken, A. R. A., et al. (2015). Ocean access to a cavity beneath Totten Glacier in East Antarctica. *Nature Geoscience*, *8*(4), 294–298. <https://doi.org/10.1038/ngeo2388>

Hogan, K. A., Larter, R. D., Graham, A. G. C., Arthern, R., Kirkham, J. D., Totten Minzoni, R., Jordan, T. A., Clark, R., Fitzgerald, V., Wåhlin, A. K., Anderson, J. B., Hillenbrand, C.-D., Nitsche, F. O., Simkins, L., Smith, J. A., Gohl, K., Arndt, J. E., Hong, J., & Wellner, J. (2020). Revealing the former bed of Thwaites Glacier using sea-floor bathymetry: implications for warm-water routing and bed controls on ice flow and buttressing. *The Cryosphere*, *14*(9), 2883–2908.

<https://doi.org/10.5194/tc-14-2883-2020>

- Howat, I. M., Porter, C., Smith, B. E., Noh, M.-J., & Morin, P. (2019). The Reference Elevation Model of Antarctica. *The Cryosphere*, *13*(2), 665–674. <https://doi.org/10.5194/tc-13-665-2019>
- Jordan, T. A., Porter, D., Tinto, K., Millan, R., Muto, A., Hogan, K., Larter, R. D., Graham, A. G. C., & Paden, J. D. (2020). New gravity-derived bathymetry for the Thwaites, Crosson, and Dotson ice shelves revealing two ice shelf populations. *The Cryosphere*, *14*(9), 2869–2882. <https://doi.org/10.5194/tc-14-2869-2020>
- Maffezzoli, N., Rignot, E., Barbante, C., Petersen, T., & Vascon, S. (2025). A gradient-boosted tree framework to model the ice thickness of the world's glaciers (IceBoost v1.1). *Geoscientific Model Development*, *18*(9), 2545–2568. <https://doi.org/10.5194/gmd-18-2545-2025>
- Millan, R., Rignot, E., Bernier, V., Morlighem, M., & Dutrieux, P. (2017). Bathymetry of the Amundsen Sea Embayment sector of West Antarctica from Operation IceBridge gravity and other data. *Geophysical Research Letters*, *44*(3), 1360–1368. <https://doi.org/10.1002/2016gl072071>
- Morlighem, M., Rignot, E., Seroussi, H., Larour, E., Ben Dhia, H., & Aubry, D. (2011). A mass conservation approach for mapping glacier ice thickness. *Geophysical Research Letters*, *38*(19), 1–6. <https://doi.org/10.1029/2011gl048659>
- Morlighem, M., Rignot, E., Mouginot, J., Seroussi, H., & Larour, E. (2014). Deeply incised submarine glacial valleys beneath the Greenland ice sheet. *Nature Geoscience*, *7*(6), 418–422. <https://doi.org/10.1038/ngeo2167>
- Morlighem, M., Williams, C. N., Rignot, E., An, L., Arndt, J. E., Bamber, J. L., et al. (2017). BedMachine v3: Complete Bed Topography and Ocean Bathymetry Mapping of Greenland From Multibeam Echo Sounding Combined With Mass Conservation. *Geophysical Research Letters*, *44*(21), 11,051–11,061. <https://doi.org/10.1002/2017gl074954>
- Morlighem, M., Rignot, E., Binder, T., Blankenship, D., Drews, R., Eagles, G., et al. (2020). Deep glacial troughs and stabilizing ridges unveiled beneath the margins of the Antarctic ice sheet. *Nature Geoscience*, *13*, 132–137. <https://doi.org/10.1038/s41561-019-0510-8>
- Mouginot, J., Rignot, E., Scheuchl, B., & Millan, R. (2017). Comprehensive Annual Ice Sheet Velocity Mapping Using Landsat-8, Sentinel-1, and RADARSAT-2 Data. *Remote Sensing*, *9*(4), 364. <https://doi.org/10.3390/rs9040364>
- Ockenden, H., Bingham, R. G., Goldberg, D., Curtis, A., & Morlighem, M. (2026). Complex mesoscale landscapes beneath Antarctica mapped from space. *Science*, *391*(6782), 314–319. <https://doi.org/10.1126/science.ady2532>
- Ockenden, H., Bingham, R. G., Curtis, A., & Goldberg, D. (2023). Ice-flow perturbation analysis: a method to estimate ice-sheet bed topography and conditions from surface datasets. *Journal of Glaciology*, *69*(278), 1677–1686. <https://doi.org/10.1017/jog.2023.50>

Rignot, E., Velicogna, I., van den Broeke, M. R., Monaghan, A., & Lenaerts, J. T. M. (2011). Acceleration of the contribution of the Greenland and Antarctic ice sheets to sea level rise. *Geophysical Research Letters*, *38*(5). <https://doi.org/10.1029/2011gl046583>

Rosier, S., H. R., Hofstede, C., Brisbourne, A. M., Hattermann, T., Nicholls, K. W., Davis, P. E. D., et al. (2018). A New Bathymetry for the Southeastern Filchner-Ronne Ice Shelf: Implications for Modern Oceanographic Processes and Glacial History. *Journal of Geophysical Research: Oceans*, *123*(7), 4610–4623. <https://doi.org/10.1029/2018jc013982>

Smith, B., Fricker, H. A., Gardner, A. S., Medley, B., Nilsson, J., Paolo, F. S., Holschuh, N., Adusumilli, S., Brunt, K., Csatho, B., Harbeck, K., Markus, T., Neumann, T., Siegfried, M. R., Zwally, H. J. (2020). Pervasive ice sheet mass loss reflects competing ocean and atmosphere processes. *Science*, *368*(6496), 1239–1242. <https://doi.org/10.1126/science.aaz5845>

Tinto, K. J., Padman, L., Siddoway, C. S., Springer, S. R., Fricker, H. A., Das, I., et al. (2019). Ross Ice Shelf response to climate driven by the tectonic imprint on seafloor bathymetry. *Nature Geoscience*, *12*(6), 441–449. <https://doi.org/10.1038/s41561-019-0370-2>

van Wessem, J. M., van de Berg, W. J., Noël, B. P. Y., van Meijgaard, E., Amory, C., Birnbaum, G., et al. (2018). Modelling the climate and surface mass balance of polar ice sheets using RACMO2 – Part 2: Antarctica (1979–2016). *The Cryosphere*, *12*(4), 1479–1498. <https://doi.org/10.5194/tc-12-1479-2018>

Young, D. A., Roberts, J. L., Ritz, C., Frezzotti, M., Quartini, E., Cavitte, M. G. P., Tozer, C. R., Steinhage, D., Urbini, S., Corr, H. F. J., van Ommen, T., & Blankenship, D. D. (2017). High-resolution boundary conditions of an old ice target near Dome C, Antarctica. *The Cryosphere*, *11*(4), 1897–1911. <https://doi.org/10.5194/tc-11-1897-2017>

## 5 DOCUMENT INFORMATION

### 5.1 Publication Date

---

January 2026

### 5.2 Date Last Updated

---

January 2026